AD NUMBER

AD058831

LIMITATION CHANGES

TO:

Approved for public release; distribution is unlimited. Document partially illegible.

FROM:

**Distribution authorized to U.S. Gov't. agencies and their contractors;
Administrative/Operational Use; MAR 1965. Other requests shall be referred to Office of Naval Research, 875 North Randolph Street, Arlington, VA 22203-1995.**

AUTHORITY

ONR ltr 26 Oct 1977

Project SQUID is a cooperative program of basic research in Jet Propulsion. It is supported jointly by the United States Army, Navy, and Air Force and is administered by the Office of Naval Research through contract Nonr-401, Task Order 111 NR-098-35.

March 1955

Technical Report PIB-25-P

PROJECT SQUID

A COOPERATIVE PROGRAM
OF FUNDAMENTAL RESEARCH
AS RELATED TO JET PROPULSION
FOR THE
OFFICE OF NAVAL RESEARCH, DEPARTMENT OF THE NAVY
OFFICE OF SCIENTIFIC RESEARCH, DEPARTMENT OF THE AIR FORCE
AND THE
OFFICE OF ORDNANCE RESEARCH, DEPARTMENT OF THE ARMY

Contract N6-ori-105, Task Order III, NR-098-038

LAMINAR PIPE FLOW WITH INJECTION AND SUCTION THROUGH A POROUS WALL

by

S. W. Yuan
Polytechnic Institute of Brooklyn

March 1955

PROJECT SQUID HEADQUARTERS
JAMES FORRESTAL RESEARCH CENTER
PRINCETON UNIVERSITY
PRINCETON, N. J.

This paper is to be presented at the meeting of the Heat Transfer and Fluid Mechanics Institute in June 1955.

LAMINAR PIPE FLOW WITH INJECTION AND SUCTION THROUGH A POROUS WALL+

By

S. W. Yuan* and A. Finkelstein**

Polytechnic Institute of Brooklyn

- - -

SUMMARY

The effect of injection and suction at the wall on the two-dimensional steady-state laminar flow of a fluid in a porous-wall pipe has been investigated in detail by the solution of the Navier-Stokes equations in cylindrical coordinates. An exact solution of the dynamic equations, reduced to a third-order nonlinear differential equation with appropriate boundary conditions, is obtained. A perturbation method was used to solve the latter equation for both small and large flows through the porous wall.

The velocity components are expressed as functions of the ratio of velocity through the porous wall to the maximum axial velocity at the pipe entrance, the coordinates of the pipe and the physical properties of the fluid.

The results show that the effect of injection at the porous wall of the pipe is to increase the friction coefficient at the wall. For an injection ratio $\frac{Q}{W} = .01$ ($500 \leq R_e \leq 2500$) the friction coefficient at the wall is increased by 70-85% over the zero injection case (Poiseuille case).

+ This research was conducted under the auspices of Project SQUID, jointly sponsored by the Office of Naval Research, Department of the Navy, Office of Scientific Research, Department of the Air Force, and Office of Ordnance Research, Department of the Army.

* Research Professor of Aeronautical Engineering.

** Research Associate of Aeronautical Engineering.

INTRODUCTION

Studies of the problem of cooling rocket and jet motors by the diffusion of fluids through porous metal combustion chamber liners have been made by means of the investigation of the boundary layer behavior along a porous plate with fluid injection [1]*. Laminar flow in a two dimensional channel with porous walls has also been investigated for extremely small suction velocity at the wall [2]. Since the problem of the flow through a porous-wall pipe with injection has not been thoroughly investigated, the purpose of this work was to obtain the basic phenomena of this type of flow which would provide a guidance for the investigation of turbulent pipe flow with injection or suction.

Another important application of the results of this study is to the boundary layer control for decreasing drag and increasing lift of airplane wings. In this connection the boundary-layer flow is sucked through the surface of the wing to a duct. The ensuing flow in the duct simulates the problem of flow through a pipe with fluid injection at the walls.

In the present investigation an exact solution of the Navier-Stokes equations in cylindrical coordinates with injection or suction as a boundary condition at the wall was obtained. On the other hand the problems of flow on a porous flat plate or curved wall were previously made by the approximate solution of the Prandtl boundary layer equations.

The assumptions made in the present study were: (1) the fluid is incompressible, i.e. the mass density and the viscosity of the fluid were assumed to be constant; (2) the main flow was assumed to be laminar, and the fluid flowing in the axial direction and the fluid flowing through the

*Numbers in brackets refer to Bibliography.

porous wall were assumed homogeneous; (3) the maximum axial velocity at the entrance of the porous-wall pipe is equal to the maximum axial velocity in the Poiseuille's flow; and (4) the fluid flowing through the porous wall is uniform throughout.

Fundamental Equations

The three-dimensional steady flow of a viscous incompressible fluid is governed by the following set of basic laws of fluid mechanics. From Newton's Second law, the Navier-Stokes equations were derived as follows:-

$$(\bar{q}\cdot\nabla)\bar{q} = -\frac{1}{\rho}\nabla p + \nu\nabla^2\bar{q} \tag{1}$$

From the principle of conservation of matter,

$$\nabla\cdot\bar{q} = 0 \tag{2}$$

If a curvilinear coordinate system is introduced with the origin at the center of the cross-section where x is taken in the direction of the flow, r in the radial direction and θ the azimuthal angle, and the ordinary vector curvilinear coordinate transformations are used, the Navier-Stokes and continuity equations become

$$u\frac{\partial u}{\partial x} + v\frac{\partial u}{\partial r} = -\frac{1}{\rho}\frac{\partial p}{\partial x} + \nu\left[\frac{\partial^2 u}{\partial r^2} + \frac{1}{r}\frac{\partial u}{\partial r} + \frac{\partial^2 u}{\partial x^2}\right] \tag{3}$$

$$u\frac{\partial v}{\partial x} + v\frac{\partial v}{\partial r} = -\frac{1}{\rho}\frac{\partial p}{\partial r} + \nu\left[\frac{\partial^2 v}{\partial x^2} + \frac{\partial^2 v}{\partial r^2} + \frac{1}{r}\frac{\partial v}{\partial r} - \frac{v}{r}\right] \tag{4}$$

and

$$\frac{\partial(ru)}{\partial x} + \frac{\partial(rv)}{\partial r} = 0 \tag{5}$$

where u and v represent the x and r components of the velocity at any point (see Fig. 1) and $\frac{\partial}{\partial \theta} = 0$ because of axially symmetric flow.

The above equations will be used to investigate the fluid flow in a circular pipe with a porous wall through which uniform fluid injection or suction is applied. The boundary conditions are

$$\text{at } r = 0: \qquad v = \frac{\partial u}{\partial r} = 0$$

$$\text{at } r = R: \qquad u = 0, \quad v = -v_0 = \text{const.} \tag{6}$$

For a two-dimensional incompressible flow a steam function exists such that

$$ru = \frac{\partial \psi}{\partial r}, \qquad -rv = \frac{\partial \psi}{\partial x} \tag{7}$$

and the continuity equation (5) is satisfied.

For a constant fluid injection or suction at the porous wall and the given boundary conditions, the following stream function is introduced:

$$\psi = \left[A + B\frac{x}{R}\right] f(\eta) \tag{8}$$

where $\eta = \left(\frac{r}{R}\right)^2$. The constant A is determined from the condition at $\eta = 0$ and $x = 0$ where the maximum velocity u_o for Poiseuille's flow exists. The constant B is determined from the law of conservation of matter. The stream function can then be expressed as:

$$\psi = \frac{R^2}{2}\left[\frac{U_0}{f'(0)} + 4V_0\frac{x}{R}\right]f(\eta) \tag{9}$$

From Eqs. (5) and (7) the velocity components in the direction of flow and the radial direction are given by

$$u = U_0\left[\frac{1}{f'(0)} + 4\frac{\lambda}{R_e}\frac{x}{R}\right]f'(\eta) \tag{10}$$

$$v = -2V_0\frac{f(\eta)}{\sqrt{\eta}} \tag{11}$$

where $\lambda = \frac{V_0 R}{\nu}$ and $R_e = \frac{U_0 R}{\nu}$. The function $f(\eta)$ appearing in the above equations is the only unknown yet to be determined in terms of the distance parameter η. Eq. (11) indicates that the radial velocity becomes a function of η only. This is because of the assumption of constant velocity v_0 at the wall.

By introducing the expressions of u and v from Eqs. (10) and (11) into the Eqs. (3) and (4) there result

$$-\frac{1}{f}\frac{\partial f}{\partial x} = \frac{4U_0}{R^2}\left[\frac{1}{f'(0)} + 4\frac{\lambda}{R_e}\frac{x}{R}\right]\left[RV_0(f'^2 - ff'') - \nu(\eta f''' + f'')\right] \tag{12}$$

$$\frac{1}{f}\frac{\partial f}{\partial \eta} = \frac{2V_0}{R}\left[RV_0\left(\frac{f'^2}{\eta^2} - \frac{2ff'}{\eta}\right) - 2\nu f'''\right] = F(\eta) \tag{13}$$

Since the right-hand side of Eq. (13) is a function of η only, differention of both sides of it with respect to x yields

$$\frac{\partial^2 f}{\partial x \partial \eta} = 0 \tag{14}$$

Hence differentiating Eq. (12) with respect to η gives

$$\frac{d}{d\eta}\left[R V_0 (f'^2 - f f'') - \nu (\eta f''' + f'') \right] = 0 \tag{15}$$

which is to be satisfied for all x.

Integrating Eq. (15), one obtains

$$\eta f''' + f'' - \lambda (f'^2 - f f'') = c \tag{16}$$

for $\lambda \leq 1$, and

$$f'^2 - f f'' - \frac{1}{\lambda} (\eta f''' + f'') = k \tag{17}$$

for $\lambda > 1$; where c and k are the constants of integration to be determined. The boundary conditions are obtained with the aid of Eqs. (6), (10) and (11). Thus:

$$f(0) = f'(1) = 0 \quad ; \quad \lim_{\eta \to 0} \sqrt{\eta}\, f''(\eta) = 0$$

$$f(1) = \frac{1}{2} \tag{18}$$

Eq. (16) is an ordinary non-linear differential equation of the third order which resulted from the Navier-Stokes equations and the continuity equation by the similarity transformation. With the aid of the four given boundary conditions an exact solution can be obtained and the constant of integration C determined.

It can be seen that the limiting form of Eq. (16), by letting V_o approach to zero, is the equation describing a flow through a circular pipe with permeable walls. The solution of this equation which satisfies all the four boundary conditions given in Eq. (18) is the well-known Poiseuille's law for pipe flow. If small values of λ are treated as a pertubation parameter a solution of Eq. (16) can be obtained which will be discussed in the next section.

On the other hand, if large values of λ are treated as a pertubation parameter the third order differential equation (17) is reduced to a second order one. The solution of Eq. (17) can also be obtained in the same manner since all four boundary conditions given in Eq. (18) can be satisfied.

SOLUTION FOR SMALL λ

The solution of Eq. (16) can be expressed for small value of λ, by a power series developed near $\lambda = 0$ as follows:

$$f = f_0 + \lambda f_1 + \lambda^2 f_2 + \cdots + \lambda^n f_n \tag{19}$$

and

$$C = C_0 + \lambda C_1 + \lambda^2 C_2 + \cdots + \lambda^n C_n \tag{20}$$

where the f_n's and C_n's are taken to be independent of λ. By substituting Eqs. (19) and (20) into Eq. (16) and equating coefficients of like powers of λ, one obtains the following set of equations:

$$\eta f_0''' + f_0'' = C_0 \tag{21}$$

$$\eta f_1''' + f_1'' + f_0'^2 + f_0 f_0'' = C_1 \tag{22}$$

$$\eta f_2''' + f_2'' - 2 f_0' f_1' + f_0'' f_1 + f_0 f_1'' = C_2$$

(23)

The boundary conditions to be satisfied by the f_n's are from Eq. (18)

$$f_n(0) = f_n'(1) = 0 \quad ; \quad \lim_{\eta \to 0} \sqrt{\eta}\, f_n''(\eta) = 0 \qquad \text{for all } n$$

$$\left.\begin{aligned} f_0(1) &= \frac{1}{2} \\ f_n(1) &= 0 \quad , \quad n \geq 1 \end{aligned}\right\}$$

(24)

The second-order perturbation solution of Eq. (16) obtained by solving Eqs. (21) to (23) is given as follows:

$$f(\eta) = \left(\eta - \tfrac{1}{2}\eta^2\right) + \lambda\left(-\frac{\eta}{18} + \frac{\eta^2}{8} - \frac{\eta^3}{12} + \frac{\eta^4}{72}\right)$$

$$+ \lambda^2\left(\frac{83}{5406}\eta - \frac{19}{540}\eta^2 + \frac{11}{432}\eta^3 - \frac{1}{144}\eta^4 + \frac{1}{720}\eta^5 - \frac{1}{10800}\eta^6\right)$$

(25)

$$C = -1 - \frac{3}{4}\lambda + \frac{11}{270}\lambda^2$$

(26)

It is seen from the above equations that the second-order perturbation solution is sufficiently accurate even for $\lambda = 1$. The velocity components in the axial and radial directions are obtained by substituting Eq. (25) into Eqs. (10) and (11), respectively as follows:

$$\frac{u}{u_o} = \left[\frac{1}{1-\frac{\lambda}{18}+\frac{83}{5400}\lambda^2} + 4\frac{\lambda}{Re}\frac{x}{R}\right]\left[1-\eta+\frac{\lambda}{36}(-2+9\eta-9\eta^2+2\eta^3)\right.$$

$$\left.+\frac{\lambda^2}{10800}(166-760\eta+825\eta^2-300\eta^3+75\eta^4-6\eta^5)\right] \tag{27}$$

$$\frac{v}{u_o} = -\frac{2\lambda}{Re\sqrt{\eta}}\left[\eta-\frac{1}{2}\eta^2+\frac{\lambda}{72}(-4\eta+9\eta^2-6\eta^3+\eta^4)\right.$$

$$\left.+\frac{\lambda^2}{10800}(166\eta-380\eta^2+275\eta^3-75\eta^4+15\eta^5-\eta^6)\right] \tag{28}$$

The pressure distribution in the axial and radial directions are obtained upon the substitution of Eq. (25) into Eqs. (12) and (13), and integrating. Then one obtains

$$\frac{p(0,0)-p(x,r)}{\rho\frac{u_o^2}{2}} = \frac{8}{Re}\left[1+\frac{3}{4}\lambda-\frac{11}{27}\lambda^2\right]\left[\frac{1}{f'(0)}+2\frac{\lambda}{Re}\frac{x}{R}\right]\left(\frac{x}{R}\right)$$

$$+4\left(\frac{\lambda}{Re}\right)^2\frac{f^2}{\eta}-\frac{8\lambda}{Re^2}[f(0)-f(\eta)] \tag{29}$$

The pressure drop in the flow direction can be readily obtained from Eq. (29), i.e.

$$\frac{p(0,r)-p(x,r)}{\rho\frac{u_o^2}{2}} = \frac{8}{Re}\left[1+\frac{3}{4}\lambda-\frac{11}{27}\lambda^2\right]\left[\frac{1}{f'(0)}+2\frac{\lambda}{Re}\frac{x}{R}\right]\left(\frac{x}{R}\right)$$

(30)

The coefficient of skin friction at the wall can also be obtained from Eq. (27), and can be written

$$C_f = \frac{\tau_o}{\rho \frac{U_o^2}{2}} = \frac{4}{Re}\left[\frac{1}{1 - \frac{\lambda}{18} + \frac{83\lambda^2}{5400}} + 4\frac{\lambda}{Re}\frac{x}{R}\right]\left[1 + \frac{\lambda}{12} - \frac{13\lambda^2}{540}\right] \tag{31}$$

SOLUTION FOR LARGE λ

The solution of Eq. (17) can be expressed for large values of λ, by a power series developed near $\frac{1}{\lambda} = 0$ as follows:

$$f = f_o + \frac{1}{\lambda} f_1 + \frac{1}{\lambda^2} f_2 + \cdots + \frac{1}{\lambda^n} f_n \tag{32}$$

and

$$k = k_o + \frac{1}{\lambda} k_1 + \frac{1}{\lambda^2} k_2 + \cdots + \frac{1}{\lambda^n} k_n \tag{33}$$

where the f_n's and k_n's are taken to be independent of λ. By substituting Eqs. (32) and (33) into Eq. (17) and setting all coefficients of like powers of $\frac{1}{\lambda}$ equal to zero, one obtains the following set of equations:-

$$f_o f_o'' - f_o'^2 = k_o \tag{34}$$

$$f_o f_1'' - 2 f_o' f_1' + f_o'' f_1 + (\eta f_o''' + f_o'') = k_1$$

$$f_o f_2'' - 2 f_o' f_2' + f_o'' f_2 + f_1 f_1'' - f_1'^2 + (\eta f_1''' + f_1'') = k_2 \tag{35}$$

(36)

The boundary conditions to be satisfied by the f_n's are from Eq. (18)

$$f_n(0) = f_n'(1) = 0 \quad ; \quad \lim_{\eta \to 0} \sqrt{\eta}\, f_n''(\eta) = 0 \quad \text{for all } n$$

$$\left.\begin{aligned} f_0(1) &= \tfrac{1}{2} \\ f_n(1) &= 0 \,, \quad n \geq 1 \end{aligned}\right\} \tag{37}$$

The first-order perturbation of Eq. (17), obtained by solving the non-linear second-order Eq. (34) and the linear second order Eq. (35), is given as follows:

$$\begin{aligned} f(\eta) = \tfrac{1}{2}\sin\tfrac{\pi}{2}\eta + \frac{1}{\lambda}\Bigg\{ & \left[A_1 - \frac{\pi^3}{16}\int_1 \frac{\eta\,\xi^2 d\xi}{\sin\frac{\pi}{2}\xi} \right]\cos\tfrac{\pi}{2}\eta \\ & + \left[A_2 - \frac{\pi^3}{16}\int_1 \frac{\eta\,\xi\, d\xi}{\sin\frac{\pi}{2}\xi} \right]\left[\tfrac{2}{\pi}\sin\tfrac{\pi}{2}\eta - \eta\cos\tfrac{\pi}{2}\eta \right] \\ & - \left[\tfrac{3}{2} + \frac{4k_1}{\pi^2}\sin\tfrac{\pi}{2}\eta \right] \Bigg\} \end{aligned} \tag{38}$$

$$k = -0.61685 - \frac{1.3253}{\lambda} \tag{39}$$

where

$$A_1 = \frac{3}{2} - \frac{\pi^3}{16}\int_0^1 \frac{\xi^2 d\xi}{\sin\frac{\pi}{2}\xi} = 0.72708$$

$$A_2 = \frac{\pi}{4} + \frac{3}{2} - \frac{\pi^3}{16}\int_1^1 \frac{\xi\, d\xi}{\sin\frac{\pi}{2}\xi} = 1.5125$$

and $k_1 = -1.3253$.

The velocity components in the axial and radial directions are obtained by substituting Eq. (38) into Eqs. (10) and (11), respectively as follows:

$$\frac{u}{u_o} = \left[\frac{1}{0.7854 + \frac{0.8437}{\lambda}} + 4 \frac{\lambda}{Re} \frac{x}{R} \right] \left[\frac{\pi}{4} \cos \frac{\pi}{2} \eta + \frac{1}{\lambda} f_1' + \cdots \right] \tag{40}$$

$$\frac{v_o}{u_o} = - \frac{2\lambda}{Re \sqrt{\eta}} \left[\frac{1}{2} \sin \frac{\pi}{2} \eta + \frac{1}{\lambda} f_1 + \cdots \right] \tag{41}$$

The pressure distribution in the axial and radial directions are obtained upon the substitution of Eq. (38) into Eqs. (12) and (13), and integrating

$$\frac{p(0,0) - p(x,r)}{\rho \frac{u_o^2}{2}} = \frac{8\lambda}{Re} \left[0.61685 + \frac{1}{\lambda} (1.3253) \right] \left[\frac{1}{f'(0)} + 2 \frac{\lambda}{Re} \frac{x}{R} \right] \left(\frac{x}{R} \right)$$

$$+ 4 \left(\frac{\lambda}{Re} \right)^2 \frac{f^2}{\eta} + 8 \frac{\lambda}{Re^2} \left[f' - f'(0) \right] \tag{42}$$

The pressure drop in the flow direction can be readily obtained from Eq. (42), i.e.

$$\frac{p(0,r) - p(x,r)}{\rho \frac{u_o^2}{2}} = 8 \frac{\lambda}{Re} \left[0.61685 + \frac{1}{\lambda} (1.3253) \right] \left[\frac{1}{f'(0)} + 2 \frac{\lambda}{Re} \frac{x}{R} \right] \frac{x}{R} \tag{43}$$

The coefficient of skin friction at the wall can also be obtained from Eq. (40), which is

$$C_f = \frac{4}{Re}\left[\frac{1}{0.7854 + \frac{0.8437}{\lambda}} + 4\frac{\lambda}{Re}\frac{x}{R}\right]\left[\frac{\pi^2}{8} + \frac{1}{\lambda}(0.1854) + \cdots\right] \tag{44}$$

DISCUSSION

The velocity distributions in the main flow direction at an arbitrary cross-section of the pipe as calculated from Eq. (27) for $\lambda = \pm 1$ and from Eq. (40) for $\lambda = 10$ are shown in Fig. 2. It was noted that when $\lambda = 0$ the profile becomes Poiseuille's paroboloid, and for $\lambda > 0$ (fluid being injected through the wall) the axial velocity increases and the velocity gradient at the wall increases. For $\lambda < 0$ (fluid being withdrawn through the wall) both the axial velocity and the velocity gradient at the wall decrease as compared with Poiseuille's case. The above phenomenum follows the law of conservation of matter. In the present case the radial velocity, which vanishes in Poiseuille's case, has a finite magnitude except at the center of the pipe where it vanishes.

In Fig. 3 the maximum velocity distributions along the axis of the pipe was shown. The increase of maximum velocity with the increase of fluid injection at the wall and decrease with suction were illustrated in Fig. 4. It was interesting to learn that for an injection ratio $\frac{V_0}{U_0} = 0.01$ ($R_e = 1000$) the maximum velocity increases about 35% over the Poiseuille's flow case.

The pressure drop in the main flow direction is shown in Fig. 5. It was found that this pressure drop became appreciably larger, even for very small fluid injection at the wall, than that in the Poiseuille's flow case, and it became appreciably less for small suction case. The ratio between the pressure drop in the radial and the axial directions is approximately equal to the injection (or suction) ratio $\frac{v_0}{u_0}$ and hence the pressure drop in the radial direction can be neglected in most practical applications.

One of the essential parameters in the present investigation is the skin friction coefficient at the wall. In Poiseuille's flow the skin friction coefficient at the wall, C_f, has a constant value of $\frac{4}{Re}$. The wall frictional coefficient as calculated from Eqs. (31) and (44) indicates that the effect of injection in a pipe flow is to increase the wall frictional coefficient and the suction to decrease the wall frictional coefficient. In a boundary-layer flow on a porous flat plate the effect of fluid injection at the wall is to increase the thickness of the boundary layer and decrease the velocity gradient at the wall, hence the wall friction decreases in this case. On the other hand in a pipe flow the effect of fluid injection at the wall is to accelerate the main stream velocity hence the velocity gradient at the wall which determines the wall friction increases. For a fluid injection ratio $\frac{v_0}{u_0} = 0.01$ the wall frictional coefficient increases by 85% over the Poiseuille's flow case. The above phenomena were shown in Figs. 6, 7 and 8. The comparison of the variation of local wall frictional coefficient with fluid injection between the case of flow in a porous-wall pipe and on a flat plate was shown in Fig. 9.

Bibliography

1, Yuan, S.W., Cooling by Protective Fluid Films, High Speed Aerodynamics and Jet Propulsion. Vol. V, Section F, being published by Princeton Press.

2, Berman, A., Laminar Flow in Channels with Porous Walls, Jour. of Applied Physics, Vol. 24, No. 3, September 1953.

3, Yuan, S.W., Project Squid Semi-Annual Progress Report, pp. 52-54, October 1, 1953.

4, McLachlan, N.W., Ordinary Non-Linear Differential Equations, Oxford Press, 1950, pp. 43-46.

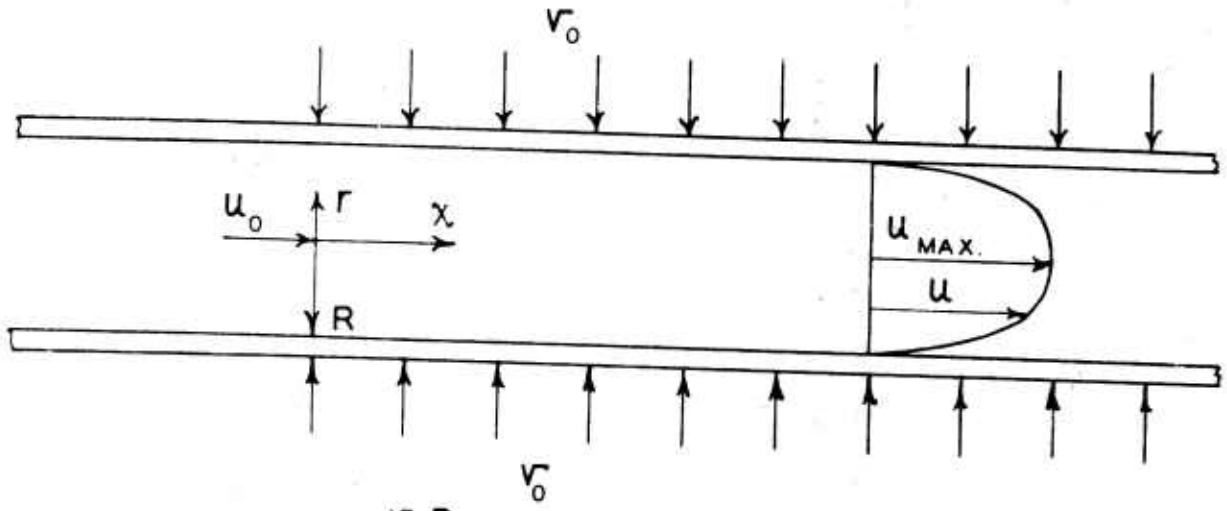

$$\lambda = \frac{V_0 R}{\upsilon} \qquad (+\lambda \text{ FOR INJECTION}, -\lambda \text{ FOR SUCTION})$$

$$R_e = \frac{u_0 R}{\upsilon}$$

FIG. 1 FLOW ALONG A POROUS PIPE WITH INJECTION

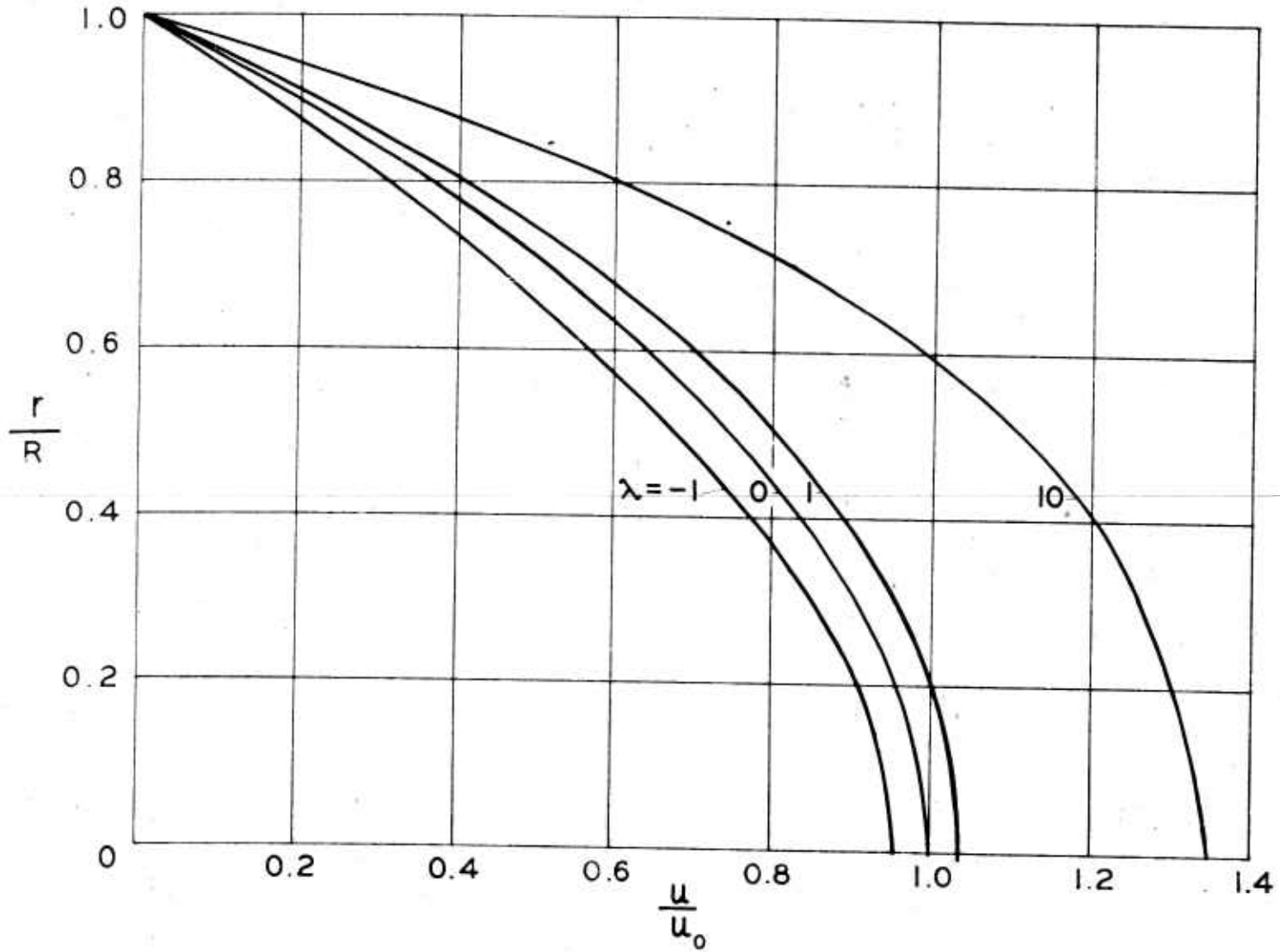

FIG. 2 VELOCITY PROFILES Vs LENGTH IN RADIAL DIRECTION FOR VARIOUS λ $\left(R_e = 10^3, \frac{x}{R} = 10\right)$

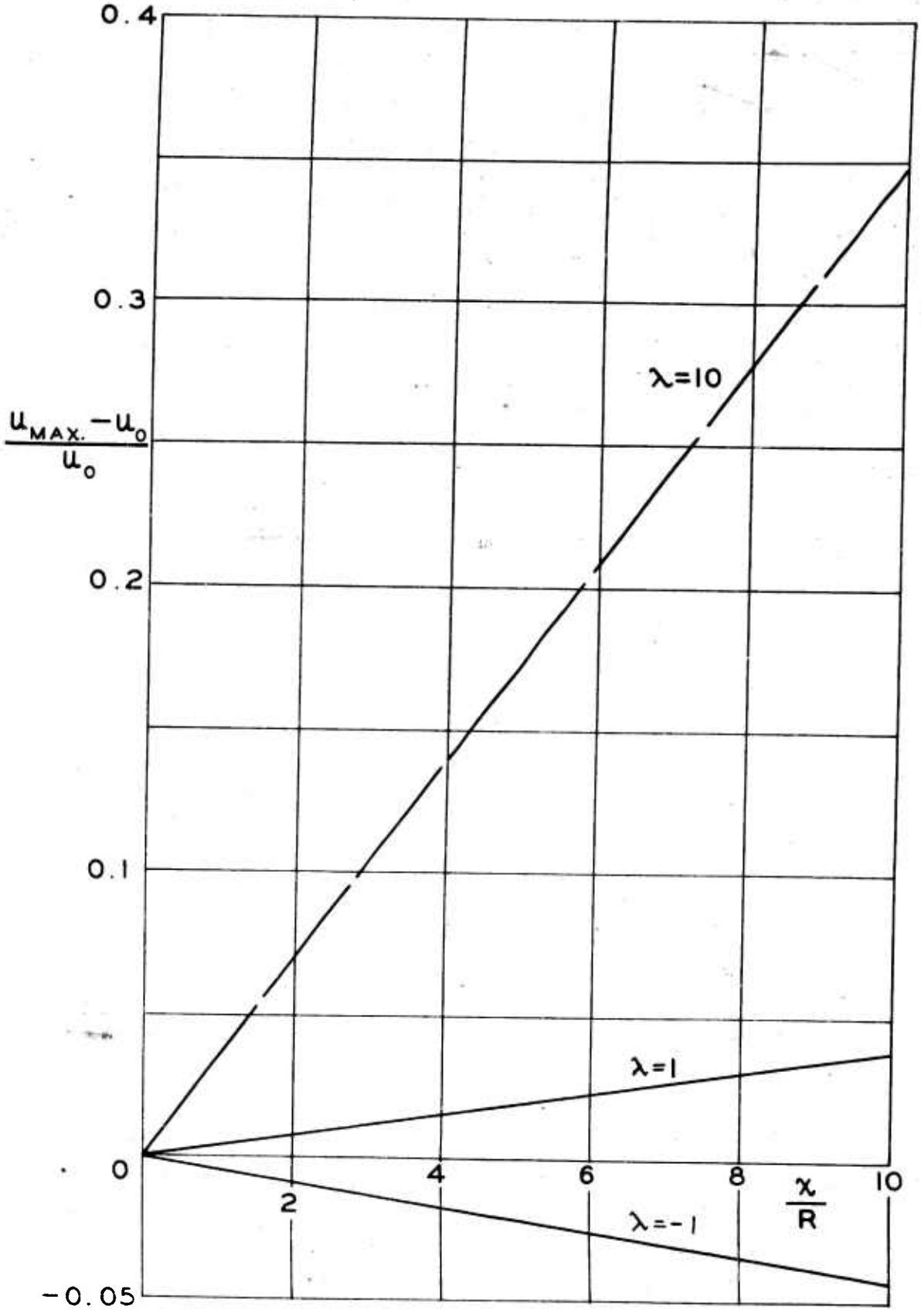

FIG. 3 MAXIMUM AXIAL VELOCITY DIFFERENCE Vs LENGTH IN THE FLOW DIRECTION ($R_e=10^3$)

FIG. 4 MAXIMUM AXIAL VELOCITY DIFFERENCE Vs INJECTION OR SUCTION RATIO $\left|\frac{V_0}{U_0}\right|$ FOR VARIOUS λ $R_e = 10^3$

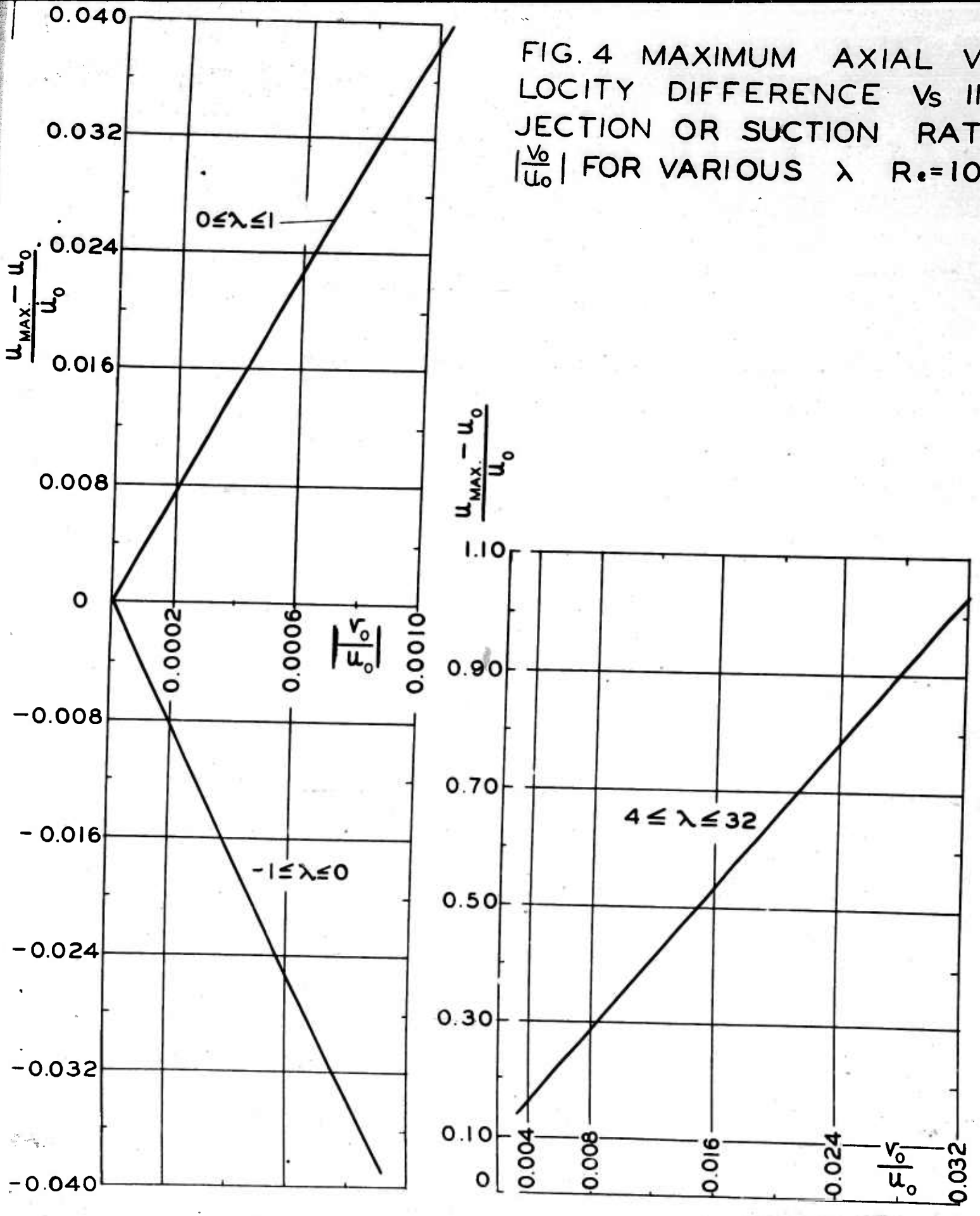

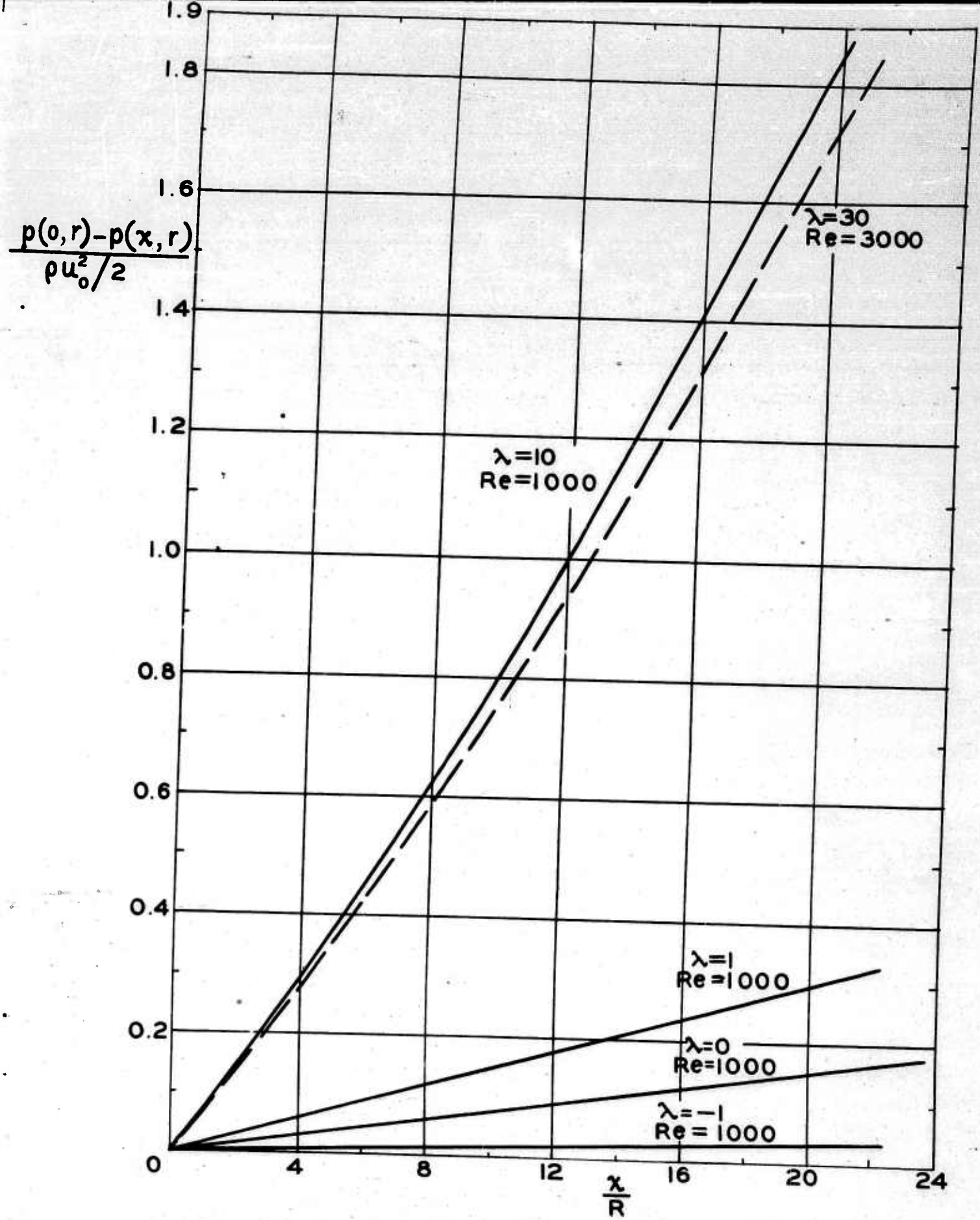

FIG. 5 AXIAL PRESSURE DROP Vs LENGTH IN FLOW DIRECTION FOR VARIOUS λ

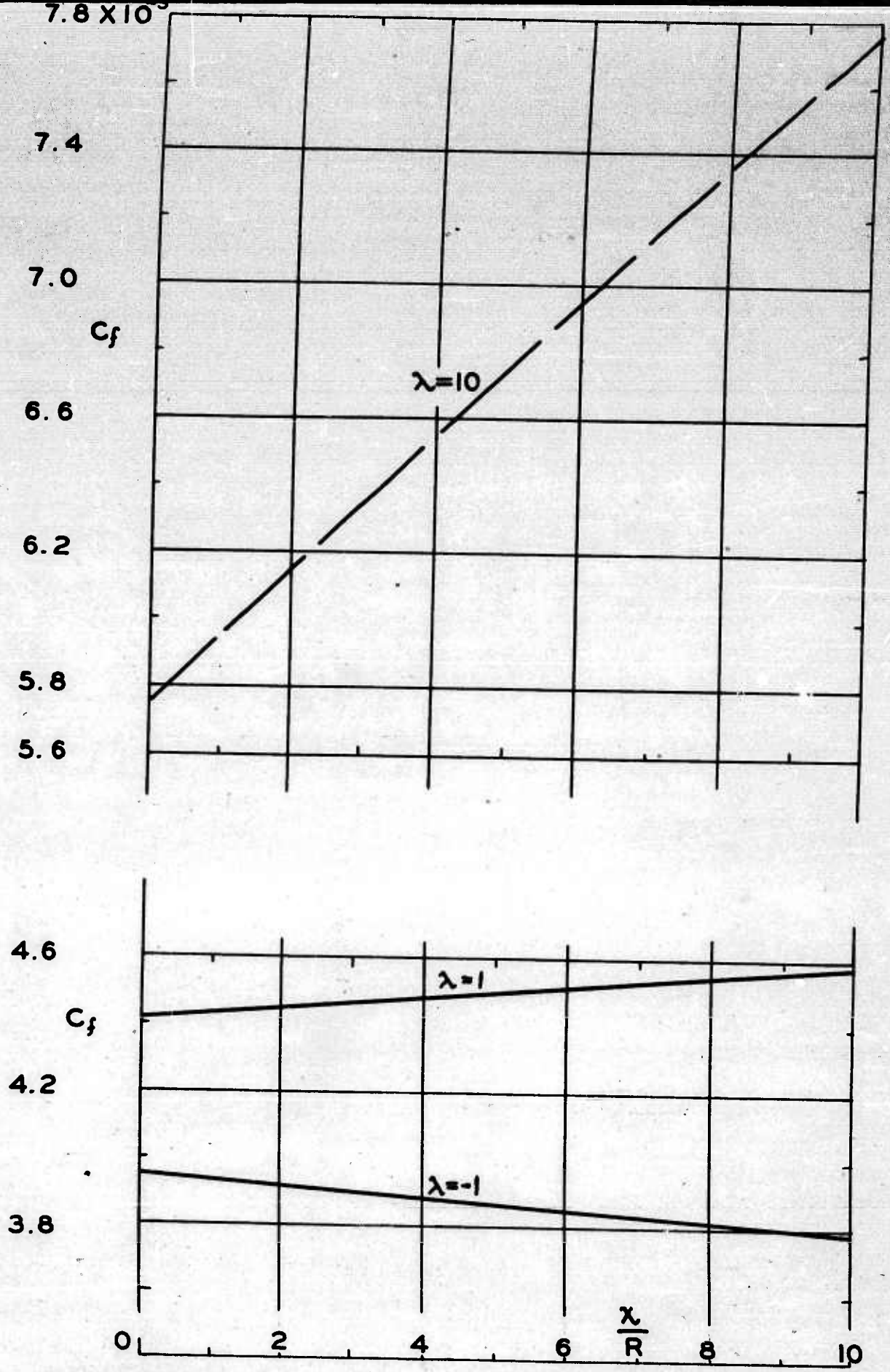

FIG. 6 VARIATION OF WALL FRICTIONAL COEFFICIENT IN FLOW DIRECTION FOR VARIOUS λ ($R_e=10^3$)

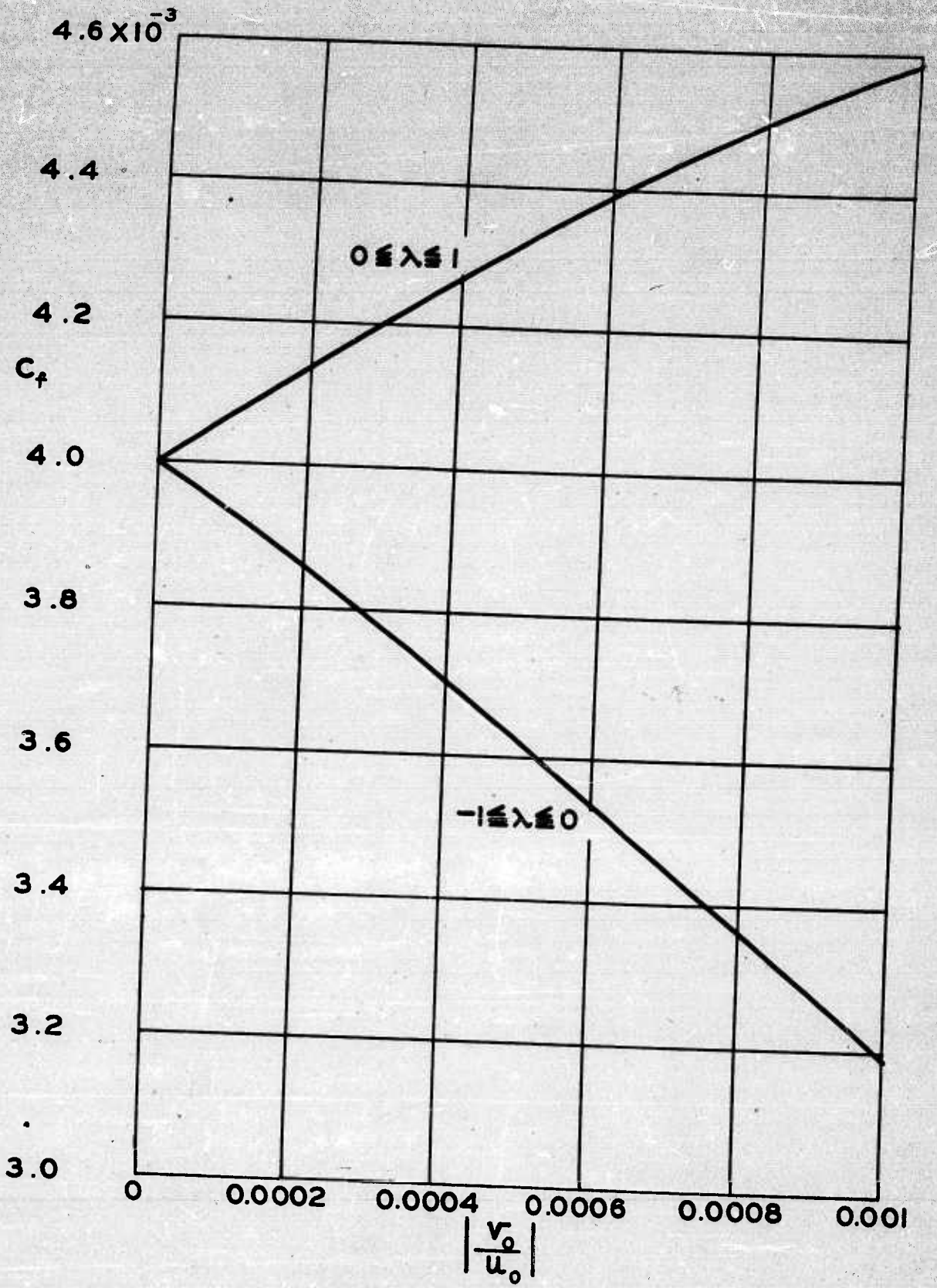

FIG.7 VARIATION OF WALL FRICTIONAL COEFFICIENT WITH INJECTION AND SUCTION RATIO FOR $-1 \leq \lambda \leq 1$

$\left(R_e = 10^3,\ \frac{x}{R} = 10\right)$

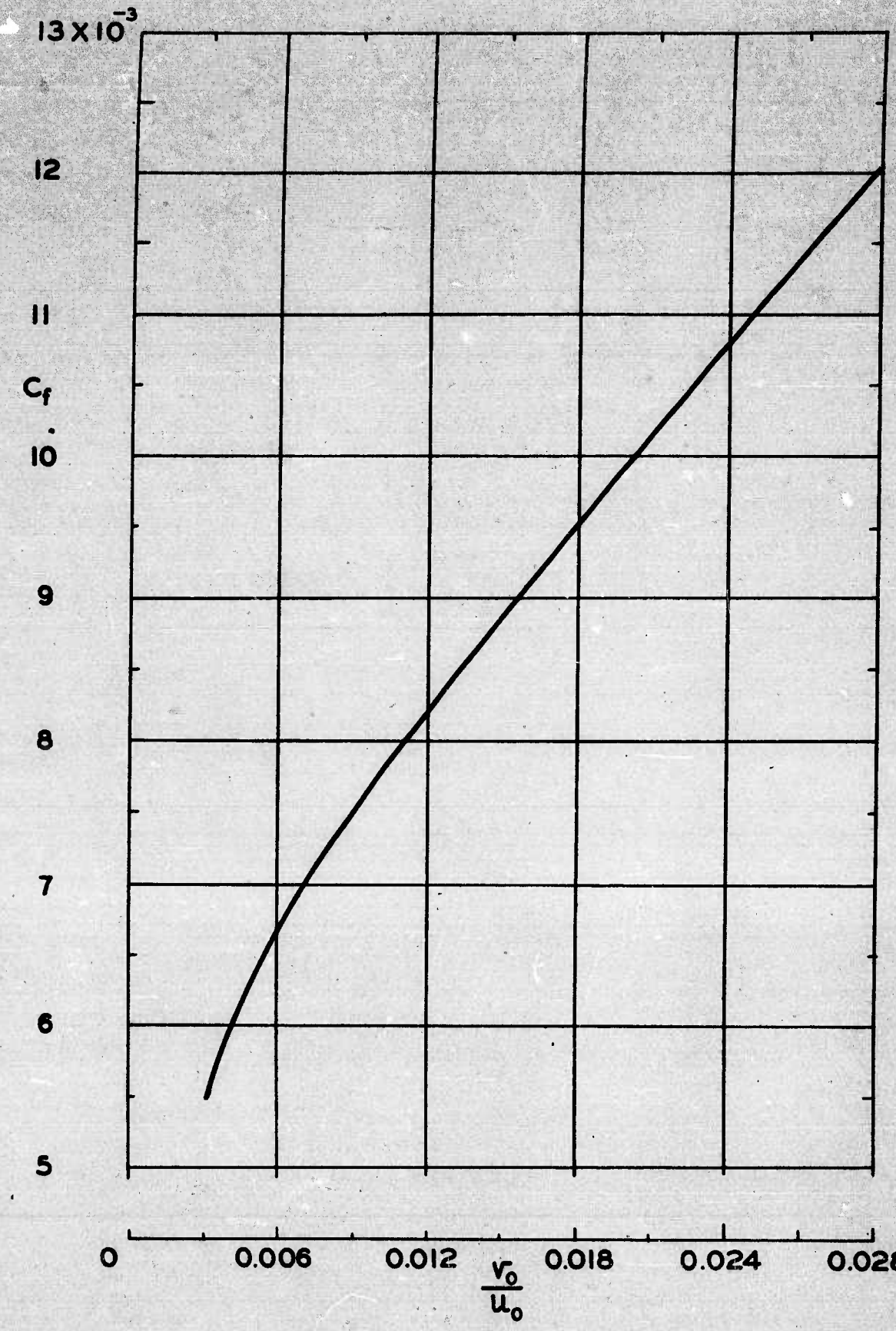

FIG. 8 VARIATION OF WALL FRICTIONAL COEFFICIENT WITH INJECTION RATIO FOR LARGE λ $(R_e = 10^3, \frac{x}{R} = 10)$

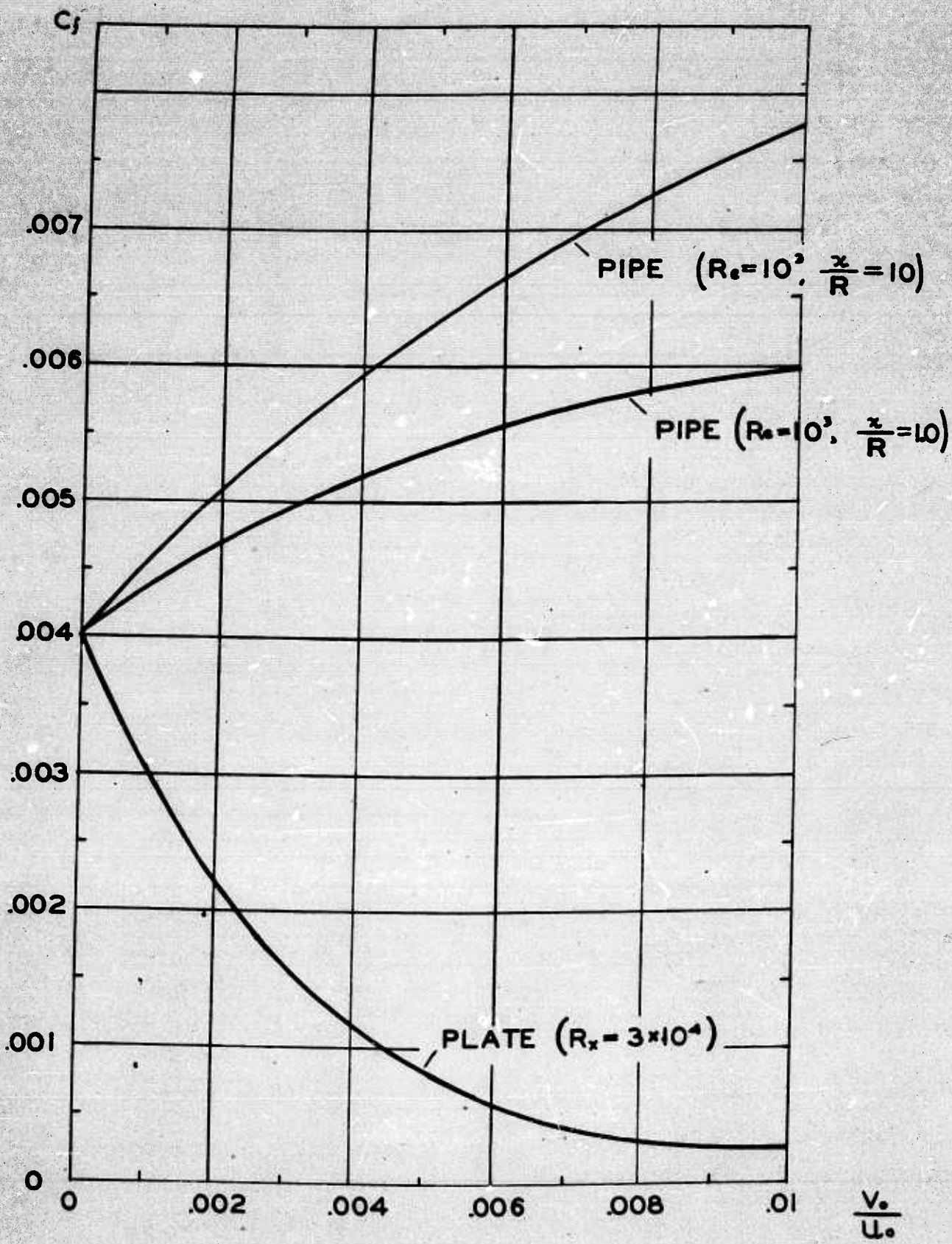

FIG. 9 VARIATION OF LOCAL WALL FRICTIONAL COEFFICIENT WITH FLUID INJECTION